Maps of foF2, hmF2, and plasma frequency above F2-layer peak in the night-time low-latitude ionosphere derived from Intercosmos-19 satellite topside sounding data

G. F. Deminova

Ann. Geophys., 25, 1827–1835, 2007
www.ann-geophys.net/25/1827/2007/

Annales Geophysicae

Maps of *fo*F2, *hm*F2, and plasma frequency above F2-layer peak in the night-time low-latitude ionosphere derived from Intercosmos-19 satellite topside sounding data

G. F. Deminova

Pushkov Institute of Terrestrial Magnetism, Ionosphere and Radio Wave Propagation, Russian Academy of Sciences (IZMIRAN), 142190 Troitsk, Moscow region, Russia

Received: 11 December 2006 – Revised: 26 June 2007 – Accepted: 26 July 2007 – Published: 29 August 2007

Abstract. Maps of *fo*F2, *hm*F2, and plasma frequency, *fp*, in the topside ionosphere at low latitudes, derived from Intercosmos-19 satellite topside sounding data, obtained from March 1979 to January 1981 and covering all longitudes, are presented for quiet geomagnetic conditions in June and December solstices at solar maximum for several local time intervals during the night. Based on these maps, features of the equatorial anomaly (EA) at different longitudes and their change during the night are considered. The maps show that averaged *fo*F2, *hm*F2, and *fp* longitudinal variations are rather complicated, their structure looks wave-like with quasi-periods in longitude of about 75–100°, similar to that on individual days revealed previously at low latitudes using Intercosmos-19 data. Positions of the structure extrema in certain longitude intervals are stable enough so that they are clearly seen in the maps after averaging over a large number of measurements made on different days and even in different years. Such structure seems to need at least five harmonics for its description.

The maps derived from Intercosmos-19 data were compared with the maps given by the IRI model. Along with general resemblance, essential distinctions between them were found. Intercosmos-19 maps show more complicated and pronounced longitudinal structure than IRI maps. They also show that at solar maximum, in general, at night, EA is stronger and persists for a longer time (on average, until 04:00 LT) than that presented in IRI model. Besides, much stronger asymmetry between the characteristics of the EA northern and southern crests in certain longitude intervals was revealed, most evident in *hm*F2 maps.

Keywords. Ionosphere (Equatorial ionosphere; Modeling and forecasting)

Correspondence to: G. F. Deminova
(deminova@izmiran.rssi.ru)

1 Introduction

Since its discovery, the equatorial anomaly (EA) has been investigated mainly in three longitude sectors: American, African, and East-Asian, where meridional chains of ground-based ionospheric stations cover both the Northern and Southern Hemispheres. It has been found that EA characteristics in these sectors differ considerably for the same local times, seasons, and latitudes – the phenomenon known as the longitudinal effect (see, e.g. Thomas, 1968; Walker, 1981). But at other longitudes the ground-based stations are very sparse and almost absent on the oceans, therefore, details of the EA structure and dynamics at those longitudes are still very uncertain, so that Rishbeth (2000) included longitude variations into a list of outstanding problems of the low-latitude ionosphere, and this problem has not been solved up to now.

Topside sounding from satellites can, to some extent, fill the data gaps. The Intercosmos-19 satellite is of interest in this respect. The unique feature of this satellite was a large onboard memory: it could record one sounding every 64 s for up to 17 h (10 orbits around the Earth) and could cover an interval of up to 250° in longitude for one observing session. The next session could begin shortly after the previous one, so that in some cases the longitude coverage was even greater. During almost two years of operation of the sounder in this regime (March 1979 to January 1981), nearly 200 such sessions were conducted that covered all longitudes, all seasons, all local times, quiet and disturbed conditions. The satellite orbit perigee and apogee were about 500 and 1000 km correspondingly; its inclination was near 74°. One revolution around the globe took about 100 min; the distance between consecutive ascending crossings of the equator was 25° in longitude, so that the local time (LT) of these crossings was almost constant with a shift of about 1 h in 5 days. With ascending and descending equator passes it took about two months to cover all local times.

Published by Copernicus Publications on behalf of the European Geosciences Union.

The Intercosmos-19 topside sounding data made it possible to conduct the most detailed analysis to date of the longitudinal variations of the ionosphere. Many unexpected findings were made using these data. For example, it was shown, for the first time, that the longitude effect, both at middle and low latitudes was much stronger than had been believed before (Kochenova, 1987, 1988, 1990; Deminov and Karpachev, 1988; Karpachev, 1988; Benkova et al., 1990). Another unexpected and surprising finding was a fairly complicated longitudinal structure of F2-layer parameters at low latitudes. Analysis of individual periods of Intercosmos-19 sounder data obtained during quiet conditions showed that at nighttime, at low latitudes, *fo*F2 and *hm*F2 longitudinal variations, in most cases, have more or less a regular wave-like character with quasi-periods of 75 to 100° in longitude and amplitudes, on average, 2 to 4 MHz and in some cases up to 8 MHz for *fo*F2 (Deminova, 1993, 1995) and, on average, 50 to 100 km, sometimes up to 200 km, for *hm*F2 (Deminova, 2002a, b). Such structures were observed in about 80% of all examined periods irrespective of season and local time, at least in the interval from 18:00 to 04:00 LT. From the analysis of all considered periods it was found that in most cases maxima and minima of the structure tend to occur in the same longitude intervals for all local times during night and in all seasons. In the June solstice the sharpest changes in *fo*F2 are observed at longitudes near 0°, with amplitudes up to 8 MHz. The deepest minimum of *fo*F2 occurs near 330°; it is observed both at the EA trough and crests and decreases beyond about 40° of the dip. At other longitudes maxima (minima) of *fo*F2 at the magnetic equator most often correspond to minima (maxima) of *fo*F2 at the EA crests and to decrease (increase) in the distance between the crests and the equator, i.e. the whole EA phenomenon shows a kind of longitudinal modulation with a quasi-period between 75° and 100° (Deminova, 2003a). Such an anti-phase pattern of *fo*F2 variations along the EA trough and crests is typical before and near midnight, but towards morning these variations sometimes become in-phase. Variations of *hm*F2 and *fo*F2 along the magnetic equator are generally in anti-phase (Karpachev, 1988; Deminova, 2002a), but at EA crests there is no clear anticorrelation between them. In the December solstice the amplitudes of this structure are somewhat smaller than in June and the minimum near 330° is not deeper than other minima. In the September equinox the pattern is more similar to that of June than of December, and in the vernal equinox it is more similar to that of December. The spatial structure of *fo*F2 longitudinal variations is usually kept rather constant during several days in succession; in individual periods the whole structure can be displaced by 10 to 20° in longitude relative to a previous day. In the region of the EA crests the amplitudes of these wave-like variations are noticeably greater than in the EA trough. Towards middle latitudes this wave-like structure gradually diminishes, disappearing beyond about 40° of the dip (Deminova, 1995). Outside the low-latitude belt the longitudinal variations of *fo*F2 may be described rather exactly by just one harmonic in the Southern and two in the Northern Hemisphere, in agreement with the results of Deminov and Karpachev (1988).

Mechanisms responsible for the formation of such detailed structure are not known up to now. The first two harmonics of the longitudinal effect can be explained by the longitude variations of the geomagnetic field declination, D. The point is that *fo*F2 is influenced by the thermospheric wind which can move ionization up to a region of weaker recombination or down to a region of stronger recombination, depending on the angle between the wind direction and the geomagnetic field; therefore, *fo*F2 at a certain point depends, among other reasons, on D (e.g. Kohl et al., 1969; Challinor and Eccles, 1971). It is well-known (e.g. Akasofu and Chapman, 1972) that the D variation along longitude can be approximated rather exactly by two harmonics in the Northern Hemisphere and near the equator and by one harmonic in the Southern Hemisphere. Just such a pattern of longitudinal variations (two harmonics in the Northern and one in the Southern Hemisphere) was observed at middle latitudes for electron density, *Ne*, in the topside ionosphere obtained with in-situ measurements from the Ariel-1 and Ariel-3 satellites (Eccles et al., 1971) and for *fo*F2 obtained from Intercosmos-19 (Deminov and Karpachev, 1988). But this mechanism cannot account for the detailed structure of the *fo*F2 and *hm*F2 changes observed at low latitudes that needs at least five harmonics for its description. Deminova (1993, 1995) assumed a multimode structure of the thermospheric winds, temperature, and composition of the thermosphere as one cause of such a structure. This supposition seems quite reasonable, as there is experimental evidence that higher harmonics of these parameters at low latitudes are rather strong (e.g. Mayr et al., 1979; Herrero and Spenser, 1982; Manson et al., 2004), but this problem requires further study.

It was revealed from Intercosmos-19 data that during the daytime the low-latitude ionosphere also has a fairly complex longitudinal structure (Kochenova, 1987, 1988, 1990). By day that structure is presumably controlled by the electric field which changes with longitude (Deminov et al., 1988; Scherliess and Fejer, 1999).

The complicated longitudinal structure is also seen in *fo*F2 maps for low latitudes derived from Intercosmos-19 data by averaging a large number of measurements and presented by Karpachev et al. (2003) for several local time (LT) intervals, 4 maps for daytime and 4 maps for the two LT intervals at nighttime for the June and December solstices. In these maps the complicated longitudinal structure is seen both by day and by nighttime.

This paper continues the investigation of the longitudinal structure of the low-latitude ionosphere. It presents 6 maps of *fo*F2 for several LT intervals during night at low latitudes for June and December solstices and in addition the maps of *hm*F2 and plasma frequency, *fp*, at a height of 500 km, derived from Intercosmos-19 data for the same LT intervals as *fo*F2. A consideration of these maps in combination made

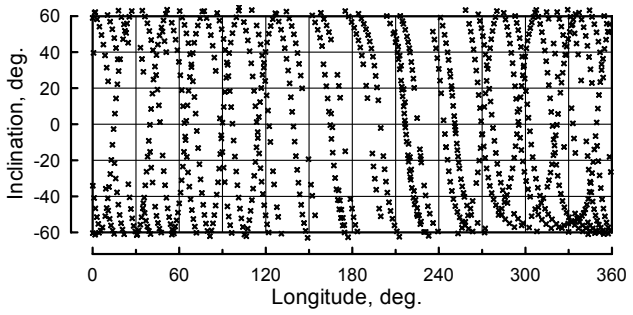

Fig. 1. The example of data coverage for the maps for 01:00–03:00 LT of the June solstice.

it possible to analyse in more detail the global structure of the low-latitude ionosphere and its evolution during night.

2 Maps of *fo*F2, *hm*F2, and *fp* in the topside ionosphere derived from Intercosmos-19 data

Using Intercosmos-19 data it is possible to construct maps of the longitudinal distribution of *fo*F2 and other ionospheric parameters based on measurements only, unlike previous mappings that compensated for the lack of data in some longitude intervals, especially over the oceans, by using so-called "screen stations" or theoretical reasoning (e.g. Jones and Gallet, 1962, 1965; Rush et al., 1983, 1984; Fox and McNamara, 1988; Bradley, 1990; Rawer, 1995; Bilitza et al., 1996; Bradley et al., 2004). In fact, Intercosmos-19 provides the possibility of reconstructing the three-dimensional distribution of *Ne* in the topside ionosphere.

In this paper maps of the distributions of *fo*F2, *hm*F2, and the plasma frequency *fp* in the topside ionosphere at a height of 500 km are presented, which were constructed on the basis of N(h)-profiles calculated from Intercosmos-19 topside ionograms. The maps are displayed for low latitudes in the magnetic dip I interval from $-60°$ up to $+60°$ for several intervals of local time in the June and December solstices, under quiet geomagnetic conditions and for solar maximum. Data obtained from mid May to August were used for June solstice maps and data from mid November to February for December solstice maps. Monthly average values of F10.7 during these periods were between 170 and 229. For each map nearly 700 to more than 1000 N(h)-profiles obtained from 1979 to 1981 were used that covered all longitudes rather uniformly. An example of the data coverage is shown in Fig. 1 for one of the LT intervals. The maps are based on a grid of 10° in inclination and 20° in longitude. A mesh size was chosen such that, on average, 1 to 6 measurements fell into each mesh. Values at the grid nodes were obtained from the measured data by interpolation based on weighting according to the square of inverse distance. For each node the data points occurring within a search ellipse with radii of 30°

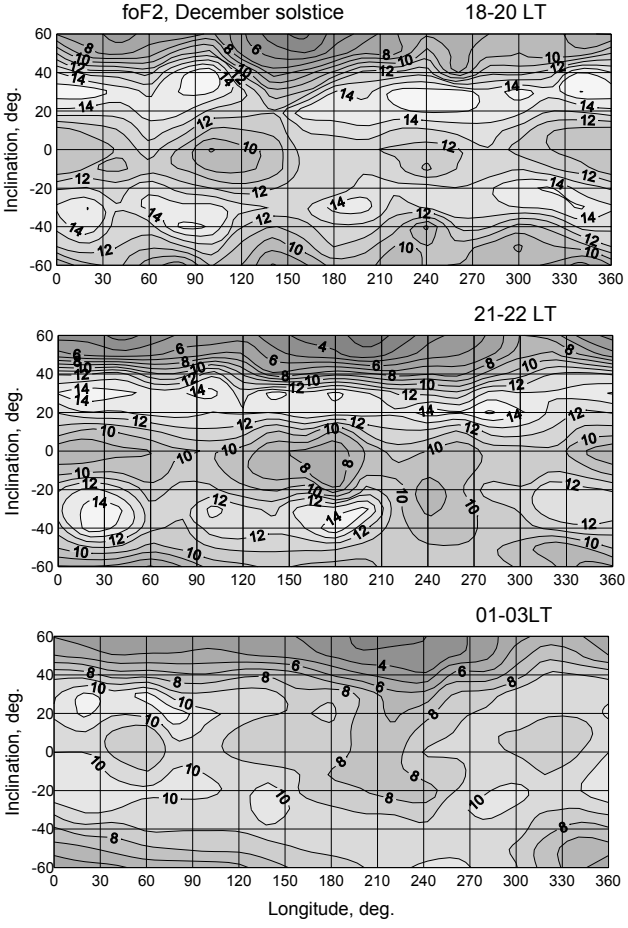

Fig. 2. Maps of *fo*F2 distribution at low-latitudes for three LT intervals in the December solstice derived from Intercosmos-19 topside sounding data.

in longitude and 15° in inclination were included. Different radii were tried, and it was found that the ellipse with radii of 20° in longitude and 10° in inclination gave practically the same maps as the above and greater ellipses, as one could expect for the given data density. But for this minimal ellipse in some LT intervals there was a small number of search areas, i.e. quadrants of the ellipse, in which no data occurred. Therefore, to avoid empty search areas the ellipse with the above radii was chosen.

Figures 2 to 7 show distributions of *fo*F2, *hm*F2, and *fp* at 500 km at low latitudes for several LT intervals at night for the December and June solstices. The three parameters are presented for all LT intervals except for 03:00–04:00 LT in the June solstice when the only data available were gathered in late May 1980 when solar activity was very high and ionograms were smeared to a greater or lesser extent by spread-F. This caused uncertainties in *hm*F2 and *fp* calculations that were too large, although in most cases, it was possible to determine *fo*F2 values with acceptable accuracy (no worse than 0.3 MHz). For all the other LT intervals there was a sufficient

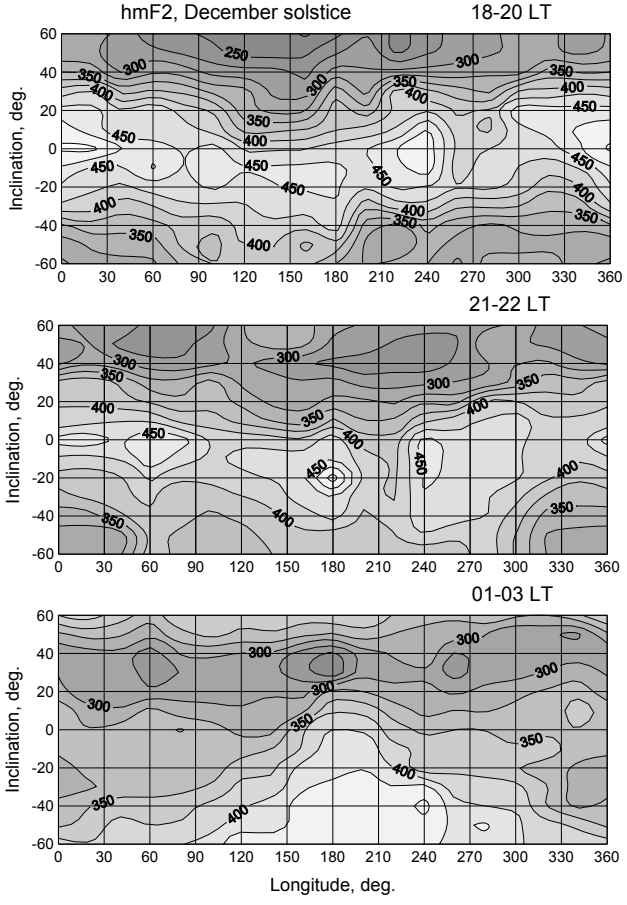

Fig. 3. The same as in Fig. 2 but for *hm*F2.

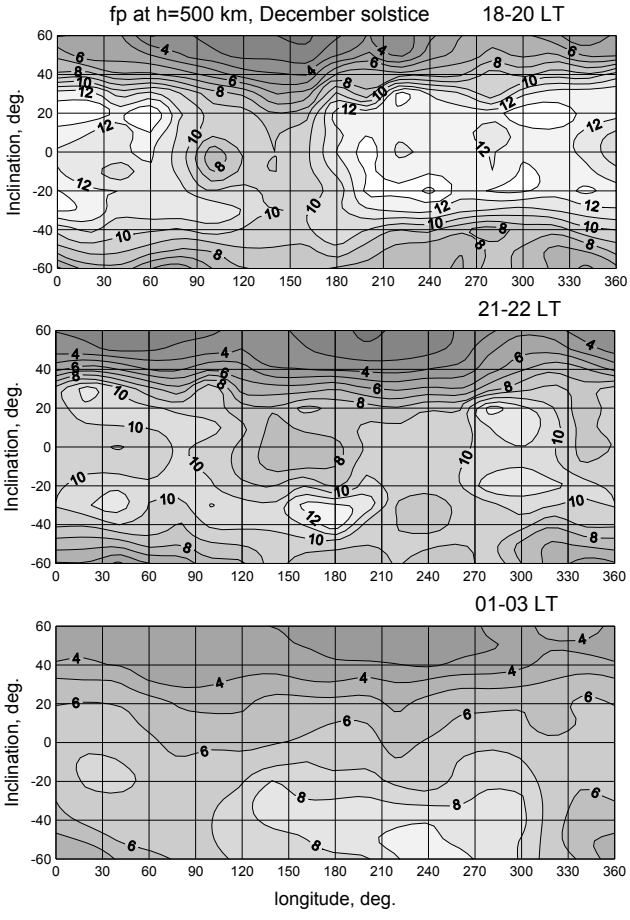

Fig. 4. The same as in Fig. 2 but for *fp* at a height of 500 km.

number of ionograms clear of spread-F that enabled the determination of *fo*F2 with an accuracy near 0.1–0.2 MHz and *hm*F2 with an accuracy near 15 km.

In Figs. 2 and 5, which show *fo*F2 maps, one can see that in both solstices before midnight the EA trough is slightly shifted relative to the magnetic equator into the summer hemisphere almost at all longitudes independently of the relative positions of the geographic and magnetic equators. This shift persists from the daytime for which this feature was described by Karpachev et al. (2003). In the *hm*F2 maps (Figs. 3 and 6) before midnight the belt of increased *hm*F2 values related to the fountain-effect is also slightly shifted relative to the magnetic equator into the summer hemisphere. After midnight this belt disappears almost at all longitudes except for the 320° to 360° interval in the both solstices and near 30° in the June solstice. During night, the EA trough is gradually shifted toward the winter hemisphere, on average, by 5° in inclination, i.e. by 2–3° in latitude, almost at all longitudes. Before midnight both EA crests are located fairly symmetrically relative to the EA trough at a mean distance of 30–35° in inclination and have approximately equal amplitudes in both solstices, with average *fo*F2 values being mainly 12 to 14 and 8 to 10 MHz in the EA crests and trough, respectively. During night both crests shift equatorward approximately from I=30–35° to 20–25°. In general, EA persists, gradually diminishing in magnitude, almost till sunrise.

In the June solstice the southern crest decays somewhat faster than the northern one. In the December solstice both crests decay with nearly the same rate everywhere except for the longitude interval approximately from 210 to 270°, where the southern crest is seen at 18:00–20:00 LT but is no longer seen in the map for 21:00–22:00 LT, and both the crests have almost disappeared in the map for 01:00–03:00 LT. Note that according to Intercosmos-19 data in individual periods the southern crest is seen quite distinctly at all longitudes, almost up to morning, but there was revealed one peculiarity. It was found that in the December solstice, at nighttime, in the region of the EA southern crest, one type of the ionization trough can occur which divides the crest top into two by a depression about 7–10° wide in latitude (Deminova, 1999). In different examples the center of this trough occurs at different latitudes within the dip latitude interval approximately from −10° to −20°. Just at longitudes from 210 to 270°

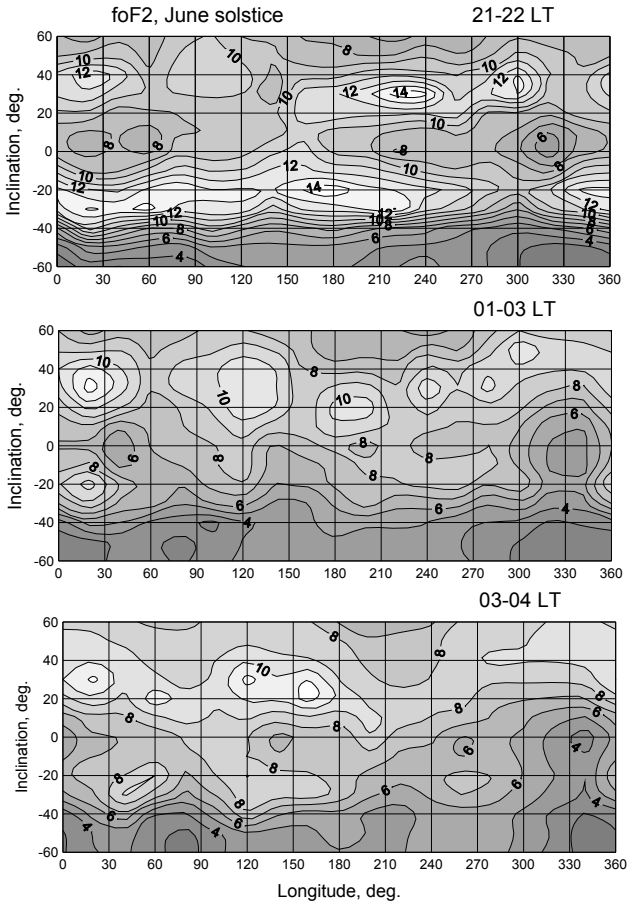

Fig. 5. The same as in Fig. 2 but for the June solstice.

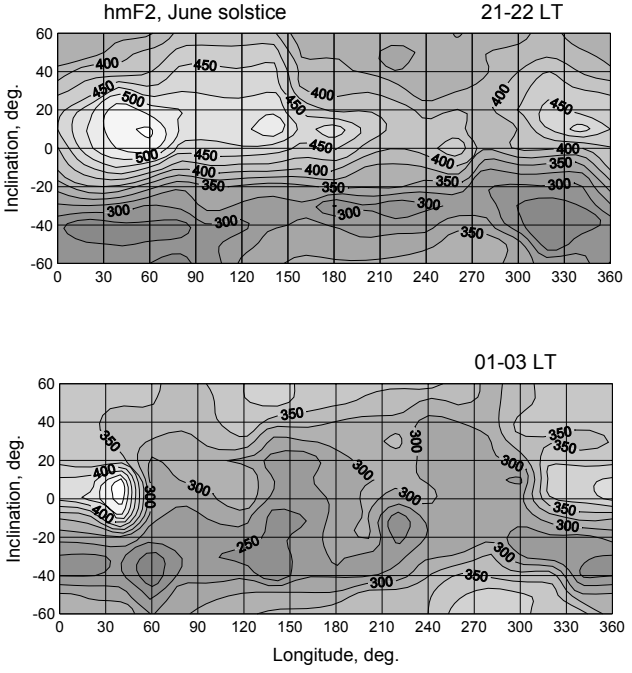

Fig. 6. The same as in Fig. 5 but for *hm*F2 and two LT intervals.

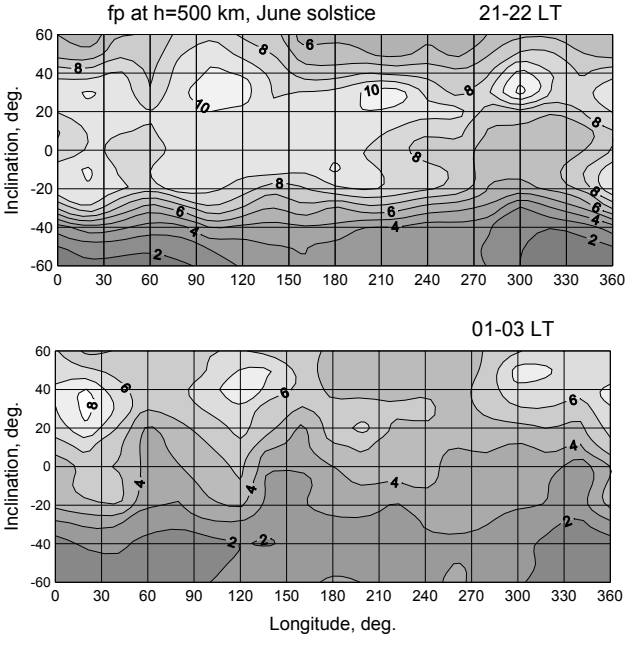

Fig. 7. The same as in Fig. 6 but for *fp* at a height of 500 km.

this trough is strongest and occurs most often (with a probability of nearly 50%), therefore, after averaging over many measurements the crest at these longitudes is smoothed out in the maps. At longitudes 330 to 30° this type of trough is observed very seldom, and the southern crest is seen in the maps quite clearly. In the June solstice similar but weaker asymmetry of the crests is seen in the *fo*F2 map for 21:00–22:00 LT at longitudes approximately from 50 to 150°, where the summer crest is considerably lower than at other longitudes. In the *hm*F2 maps for 21:00–22:00 LT in those longitude intervals in the December and June solstices, respectively, the F2-layer height in the region of the EA summer crest is noticeably higher than at other longitudes, suggesting that the wind from the summer hemisphere to the winter one is stronger at those longitudes. However, after midnight in the June solstice *hm*F2 values in the longitude interval 50 to 150° differ only slightly from those at other longitudes. By contrast, in the December solstice the region with increased *hm*F2 values at longitudes of about 150 to 280° becomes even more prominent after midnight. This region is not yet seen in the map for 18:00–20:00 LT. It begins to form at 21:00–22:00 LT and is most pronounced after midnight, covering the area from the equator to midlatitudes of the Southern Hemisphere. Such *fo*F2 and *hm*F2 dynamics suggests that at night the wind from the Southern (summer) Hemisphere to the Northern one in December is considerably stronger than from the Northern Hemisphere to the Southern one in June, at least at the longitudes specified above, and this

asymmetry between the hemispheres is apparently stronger than shown in the neutral wind model HWM93 (Hedin et al., 1996). This suggestion is also supported by the fact that the above-mentioned trough occurs often at the southern crest in December but very occasionally at the northern crest in June. The characteristics of this trough are evidence that its cause is just the thermospheric wind blowing from the summer hemisphere to the winter one that lifts ionization upwards along the geomagnetic field lines, and if this wind is strong enough it can reduce the density, *Ne*, at the *hm*F2 level. The observations agree well with model calculations of wind influence on *Ne* distribution (Anderson et al., 1981).

In the maps of *fp* distribution at 500 km (Figs. 4 and 7) before midnight the EA is distinctly seen in the December solstice almost at all longitudes but in the June solstice only at certain longitude intervals. After midnight the EA is not seen at this height, but *fp* values are still higher in the summer crest region. In the maps for 600 and 700 km (not shown in this paper) the EA is not seen, but increased *fp* values are observed at the EA summer crest. With increasing height the belt of increased *fp* values is shifted towards the magnetic equator. In general, *fp* distribution above F2-layer peak derived from Intercosmos-19 data is consistent with that obtained with in-situ *Ne* measurements by other satellites: Ariel-3 at about 550 km (Hopkins, 1972) and Hinotori at 600 km (Su et al., 1996).

The maps presented show that even averaged over a large number of measurements *fo*F2, *hm*F2, and *fp* variations along the EA crests and trough are rather complicated. They have a wave-like form with a quasi-period of about 75–100° along longitude, similar to that on individual days, but, of course, with smaller amplitude. It is obvious that due to the limited amount of data, a few of the features seen in the maps may be atypical. This is especially true for the 18:00–20:00 LT maps, as at that local time interval the equatorial F2-layer height can change very rapidly. Despite this, the general structure shown in the maps has consistency. The minima and maxima of this structure are located at more or less similar longitude intervals both before and after midnight, although the measurements used for these maps were made on different days and even in different years. This is evidence for the relative stability of such a longitudinal structure in time. The maps show that the amplitudes of these averaged longitudinal variations are about 2 MHz for *fo*F2 and *fp*, and about 50 km for *hm*F2. For *fo*F2 and *fp* this amplitude is sufficiently greater than other expected changes in these values in the maps (related, for example, with the difference in F10.7 values at periods used for the maps), therefore, this structure in the averaged pattern is fairly reliable. The excess is not very big for *hm*F2, therefore, such averaged variations in *hm*F2 maps should be considered only as a tendency. Recall that on individual days the *hm*F2 variations with quasi-periods of 75–100° have amplitudes of about 100 km, which is much greater than the uncertainty in the determination of *hm*F2, i.e. they are quite reliable. Stronger smoothing of the *hm*F2 variations after averaging occurs presumably because *hm*F2 values at low latitudes are more responsive than *fo*F2 to even a weak disturbance, for example, in the electric fields, which play a very important role in the dynamics of the low-latitude ionosphere (Fejer, 1997).

The *fo*F2 longitude variations with quasi-periods of 75–100° are generally more pronounced in the summer hemisphere than in the winter one. They are seen distinctly in the maps both in the region of the summer EA crest and along the magnetic equator. These variations are also observed in the topside ionosphere at the heights up to at least 700 km. They are seen in Figs. 4 and 7, more clearly for the June solstice. The longitudinal variations in *hm*F2 with such periods are more evident in the maps for the June solstice, where they are more pronounced after midnight both along the magnetic equator and at latitudes of both the EA crests. In the December solstice such *hm*F2 variations are clearly defined at latitudes of the EA Northern (winter) crest; they are much weaker (almost at the level of uncertainty in the values of *hm*F2) along the magnetic equator, and are almost not apparent in the Southern (summer) Hemisphere. In the *hm*F2 maps for both solstices one more peculiar feature is seen, namely, small areas of strongly reduced *hm*F2 values that stand out distinctly in the winter hemispheres at I values near to 30–40°. Note that from all examined individual orbits, lowest *hm*F2 values were found at the orbit segments passing just through those areas, so this feature in the maps is not random.

3 Discussion

Intercosmos-19 maps for *fo*F2, *hm*F2, and *fp* in the topside ionosphere presented in this paper show a complicated longitudinal structure of these parameters at low latitudes. In the Introduction evidence was presented that such a small-scale, wave-like structure is an inherent feature of the low-latitude ionosphere. Amplitudes of *fo*F2, *fp*, and *hm*F2 longitudinal variations with quasi-periods of 75 to 100° at low latitudes on individual days are so big and positions of their extrema in certain longitude intervals are so stable that they are clearly seen in the maps after averaging over a large number of measurements made on different days and even in different years.

Such small-scale structure is absent in the IRI-URSI *fo*F2 maps. In the paper by Karpachev et al. (2003) several *fo*F2 maps for different LT intervals made using Intercosmos-19 data with the same method as that described above have been compared with corresponding IRI-URSI maps. As one could expect, the comparison showed that the general features of the *fo*F2 distribution obtained from Intercosmos-19 are similar to the IRI-URSI maps. But essential differences have also been revealed, most prominent of which is a much more complicated longitudinal structure of *fo*F2 variations. URSI coefficients for *fo*F2 were calculated with regard to *fo*F2 maps constructed on the basis of ISS-b satellite topside sounding

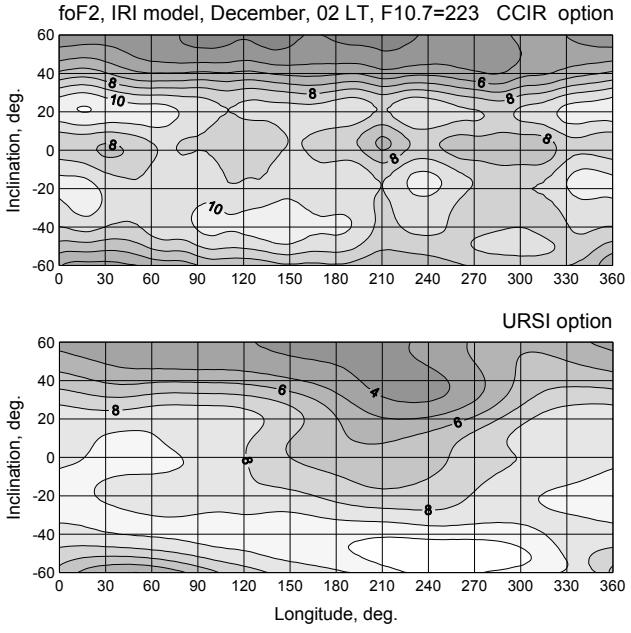

Fig. 8. IRI *fo*F2 maps with URSI and CCIR coefficients for 02:00 LT in the December solstice.

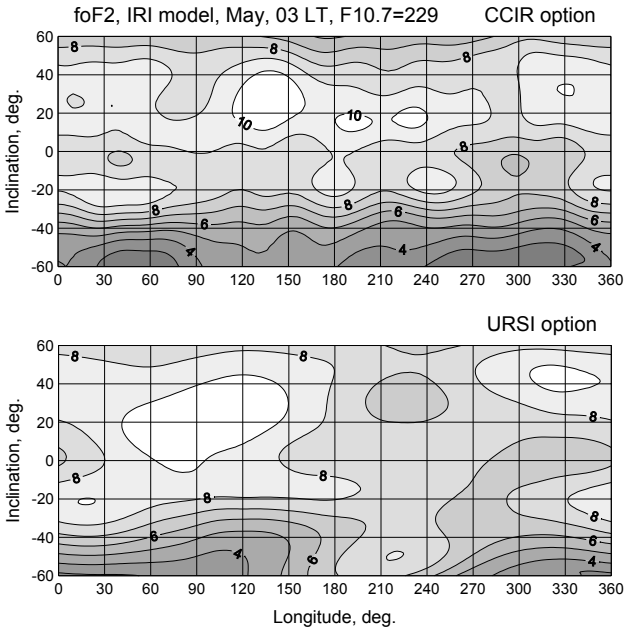

Fig. 9. IRI *fo*F2 maps with URSI and CCIR coefficients for 03:00 LT in the June solstice.

(Fox and McNamara, 1988). ISS-b was launched in 1978, its operations overlapped with Intercosmos-19 and also occurred in solar maximum. It had an onboard tape recorder that could store data for up to 115 min, i.e. a little longer than one revolution around the globe, so it could carry out measurements at any longitude and then transmit them to a ground station when passing in its vicinity (Matuura, 1979). Thus, ISS-b measurements covered all longitudes, similar to Intercosmos-19. But the method of deriving *fo*F2 maps from ISS-b data was different from that described above for Intercosmos-19. ISS-b maps were derived using the spherical surface harmonic expansion method with just two harmonics being used to account for *fo*F2 longitudinal variations in the constant local time (LT) maps (Matuura, 1979). Therefore, ISS-b maps do not reproduce the small-scale longitudinal structure revealed with Intercosmos-19 data and seen in its maps and which apparently needs at least five harmonics for its description.

The structure of the IRI *fo*F2 maps at low latitudes obtained using the CCIR coefficients was found to be somewhat closer to the Intercosmos-19 maps. As an illustration, Figs. 8 and 9 show the IRI-URSI and CCIR *fo*F2 maps for F10.7 values averaged over the months when data were gathered for the Intercosmos-19 maps for 01:00–03:00 LT of the December solstice and for 03:00–04:00 LT of the June solstice correspondingly. Comparison of Fig. 8 with Fig. 2 and Fig. 9 with Fig. 5 shows that the IRI-CCIR maps agree with the Intercosmos-19 maps for low latitudes a little better in *fo*F2 structure. Note that Intercosmos-19 data for *fo*F2 in individual periods also agree with CCIR somewhat better than with the URSI option (Deminova, 2003b).

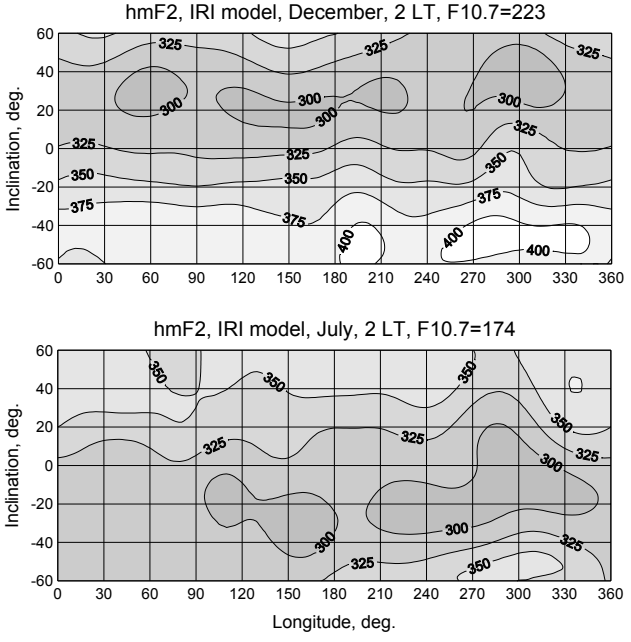

Fig. 10. IRI *hm*F2 maps for 02:00 LT in the December and June solstices.

The maps of *hm*F2 derived from Intercosmos-19 data, while showing a general resemblance to the IRI model, also exhibit essential differences. Figure 10 shows two IRI *hm*F2 maps for F10.7 values averaged as above, corresponding to the Intercosmos-19 maps for 01:00–03:00 LT of the December solstice and for 01:00–03:00 LT of the June solstice. As is

well-known, for the non-sunlit ionosphere the IRI CCIR and URSI options give practically the same *hm*F2 values, as both are based on the CCIR coefficients for M(3000)F2 (Bilitza, 2001). From a comparison of Fig. 10 with Figs. 3 and 6 it is seen that magnitudes of *hm*F2 longitudinal and latitudinal changes in the Intercosmos-19 maps are considerably greater than in the IRI maps. Besides, in the Intercosmos-19 map for 01:00–03:00 LT of the December solstice it is clearly seen that *hm*F2 values in the vast region of longitudes from 150 to 300° in the Southern Hemisphere are much higher than at other longitudes, while the IRI map does not reproduce this feature. In the Intercosmos-19 map for 01:00–03:00 LT of the June solstice a similar longitudinal peculiarity is barely evident.

Thus, Intercosmos-19 data provide evidence that the structure of the low-latitude ionosphere is much more complicated than represented in the IRI model and is far from being thoroughly investigated. It would be very interesting to compare Intercosmos-19 results with other topside sounding data which also cover all longitudes. As far as we know, the only such data are ISS-b data. But ISS-b results were published only in the form of *fo*F2 maps based on combining together a large number of measurements, and original ionograms are not available. Satellites with modern equipment, with capabilities far exceeding those of almost thirty years ago, could provide enough measurements both for refinement of Intercosmos-19 results and for producing more adequate ionospheric models.

4 Conclusions

In this paper maps of *fo*F2, *hm*F2, and plasma frequency *fp* in the topside ionosphere at low latitudes, derived from Intercosmos-19 satellite topside sounding data, obtained from March 1979 to January 1981 and covering all longitudes, are presented for quiet geomagnetic conditions in the June and December solstices in solar maximum for several local time intervals during the night. Based on these maps, features of EA at different longitudes and their change during the night are considered. The maps show that averaged *fo*F2, *hm*F2, and *fp* longitudinal variations are rather complicated, their structure looks wave-like with quasi-periods in longitude of about 75–100°, similar to that observed previously on individual days at low latitudes with Intercosmos-19 data and briefly described in the Introduction. This satellite data is evidence that such a small-scale, wave-like structure is an inherent feature of the low-latitude ionosphere. The main characteristics of this structure suggest an important role in its formation of the higher harmonic structure of the thermospheric winds, temperature, and composition of the thermosphere. Positions of the structure extrema in certain longitude intervals are stable enough, so that they are clearly seen in the maps derived after averaging over a large number of measurements made on different days and even in different years. Such a structure seems to need at least five harmonics for its description.

The maps derived from Intercosmos-19 data were compared with maps derived using the IRI model. Along with a general resemblance, essential differences between the maps were found. Intercosmos-19 maps show more complicated and pronounced longitudinal structure than IRI maps. They also show that, in general, at night, EA is stronger and persists for a longer time (on average, until 04:00 LT) than presented in the IRI model. In addition, much stronger asymmetry between characteristics of the EA northern and southern crests in certain longitude intervals was revealed, most evident in the *hm*F2 maps.

Acknowledgements. This work was supported by the Russian Foundation for Basic Research, project # 04-05-64908. The author is grateful to A. T. Karpachev for helpful discussions and to V. H. Depuev for help in producing the IRI maps.

Topical Editor M. Pinnock thanks P. L. Dyson and another anonymous referee for their help in evaluating this paper.

References

Akasofu, S.-I. and Chapman, S.: Solar-Terrestrial Physics, Clarendon Press, Oxford, 1972.

Anderson, D. and Roble, R. G.: Neutral wind effects on the equatorial F-region ionosphere, J. Atmos. Terr. Phys., 43, 835–843, 1981.

Benkova, N. P., Deminov, M. G., Karpachev, A. T., Kochenova, N. A., Kushnerevsky, Yu. V., Migulin, V. V., Pulinets, S. A., and Fligel, M. D.: Longitude features shown by topside sounder data and their importance in ionospheric mapping, Adv. Space Res., 10, 57–66, 1990.

Bilitza, D.: International Reference Ionosphere 2000, Radio Sci., 36, 261–275, 2001.

Bilitza, D., Koblinsky, C., Zia, S., Williamson, R., and Beckley, B.: The equator anomaly region as seen by the TOPEX/Poseidon satellite, Adv. Space Res., 18, 23–32, 1996.

Bradley, P. A.: Mapping the critical frequency of the F2-Layer: Part 1 – Requirements and developments to around 1980, Adv. Space Res., 10, 47–56, 1990.

Bradley, P. A., Stanislawska, I., and Juchnikowski, G.: Perspectives on updated *fo*F2 maps for IRI, Adv. Space Res., 34, 2067–2074, 2004.

Challinor, R. A. and Eccles, D.: Longitudinal variations of the mid-latitude ionosphere produced by neutral-air winds – 1. Neutral air winds and ionospheric drifts in the northern and southern hemispheres, J. Atmos. Terr. Phys., 33, 363–369, 1971.

Deminov, M. G. and Karpachev, A. T.: Longitudinal effect in the night-time mid-latitude ionosphere as given by the "Intercosmos-19" data, Geomagn. Aeronomy (in Russian), 28, 76–80, 1988.

Deminov, M. G., Kochenova, N. A., and Sitnov, Yu. S.: Longitudinal variations of electric field in the equatorial ionosphere, Geomagn. Aeronomy (in Russian), 28, 71–75, 1988.

Deminova, G. F.: Wave-like structure of longitudinal variations of the night-time equatorial ionosphere, Geomagn. Aeronomy (in Russian), 33, 167–169, 1993.

Deminova, G. F.: Wave-like structure of longitudinal variations of the night-time equatorial anomaly, Geomagn. Aeronomy (in Russian), 35, 169–173, 1995.

Deminova, G. F.: One type of the low-latitude trough of the ionization in the Southern hemisphere, Adv. Space Res., 24, 1503–1506, 1999.

Deminova, G. F.: Asymmetry of the longitudinal effect in the low-latitude ionosphere, Adv. Space Res., 29, 911–915, 2002a.

Deminova, G. F.: Variations of the altitude-longitudinal characteristics of the equator anomaly during night, Geomagn. Aeronomy (in Russian), 42, 771–779, 2002b.

Deminova, G. F.: Fine structure of *fo*F2 longitudinal distribution in the night-time low-latitude ionosphere derived from Intercosmos-19 topside sounding data, Adv. Space Res., 31, 531–536, 2003a.

Deminova, G. F.: Comparison of the *fo*F2 longitude distribution in the night-time low-latitude ionosphere inferred from Intercosmos-19 data with IRI and ground-based data, Geomagn. Aeronomy (in Russian), 43, 377–381, 2003b.

Eccles, D., King, J. W., and Rothwell, P.: Longitudinal variations of the mid-latitude ionosphere produced by neutral-air winds – 2. Comparisons of the calculated variations of electron concentration with data obtained from the Ariel 1 and Ariel 3 satellites, J. Atmos. Terr. Phys., 33, 371–377, 1971.

Fejer, B. G.: The electrodynamics of the low latitude ionosphere: recent results and future challenges, J. Atmos. Terr. Phys., 59, 1465–1482, 1997.

Fox, M. W. and McNamara, L. F.: Improved world-wide maps of monthly median *fo*F2, J. Atmos. Terr. Phys., 50, 1077–1086, 1988.

Hedin, A. E., Fleming, E. L., Manson, A. H., Schmidlin, F. J., Avery, S. K., Clark, R. R., Franke, S. J., Fraser, G. J., Tsuda, T., Vial, F., and Vincent, R. A.: Empirical wind model for the upper, middle and lower atmosphere, J. Atmos. Terr. Phys., 58, 1421–1447, 1996.

Herrero, F. A. and Spenser, N. W.: On the horizontal distribution of the equatorial thermosphere midnight temperature maximum and its seasonal variation, Geophys. Res. Lett., 9, 1179–1182, 1982.

Hopkins, H. D.: Longitudinal variation of the equatorial anomaly, Planet. Space Sci., 20, 2093–2098, 1972.

Jones, W. B. and Gallet, R. M.: The representation of diurnal and geographic variations of ionospheric data by numerical methods, Telecomm. J., 29, 129–149, 1962.

Jones, W. B. and Gallet, R. M.: The representation of diurnal and geographic variations of ionospheric data by numerical methods (Pt.2), Telecomm. J., 32, 18–28, 1965.

Karpachev, A. T.: Characteristics of the global longitudinal effect in the night-time equatorial anomaly, Geomagn. Aeronomy (in Russian), 28, 46–49, 1988.

Karpachev, A. T., Deminova, G. F., Depuev, V. H., and Kochenova, N. A.: Diurnal variations of the peak electron density distribution pattern at low latitudes derived from Intercosmos-19 topside sounding data, Adv. Space Res., 31, 521–530, 2003.

Kochenova, N. A.: Longitudinal variations of the equatorial ionosphere according to Intercosmos-19 data, Geomagn. Aeronomy (in Russian), 27, 142–144, 1987.

Kochenova, N. A.: Longitudinal variations of N(h) profiles at the magnetic equator, Geomagn. Aeronomy (in Russian), 28, 144–146, 1988.

Kochenova, N. A.: Longitudinal variations of the day-time equatorial ionosphere inferred from Intercosmos-19 data, Adv. Space Res., 10, 67–70, 1990.

Kohl, H., King, J. W., and Eccles, D.: An explanation of the magnetic declination effect in the ionospheric F2-Layer, J. Atmos. Terr. Phys., 31, 1011–1016, 1969.

Manson, A. H., Meek, C., Hagan, M., Zhang, X., and Luo, Y.: Global distributions of diurnal and semidiurnal tides: observations from HRDI-UARS of the MLT region and comparisons with GSWM-02 (migrating, nonmigrating components), Ann. Geophys., 22, 1529–1548, 2004, http://www.ann-geophys.net/22/1529/2004/.

Matuura, N. (Ed.): Atlas of ionospheric critical frequency (*fo*F2) obtained from Ionosphere Sounding Satellite-b observation, Part 1, August to December 1978, Radio Research Lab., Ministry of Posts and Telecommunications, Japan, 1979.

Mayr, H. G., Harris, I., Spenser, N. W., Hedin, A. E., Wharton, L. E., et al.: Atmospheric tides and the midnight temperature anomaly, Geophys. Res. Lett., 6, 447–450, 1979.

Rawer, K.: Ionospheric mapping in the polar and equatorial zones, Adv. Space Res., 16, 9–12, 1995.

Rishbeth, H.: The equatorial F-layer: progress and puzzles, Ann. Geophys., 18, 730–739, 2000, http://www.ann-geophys.net/18/730/2000/.

Rush, C. M., PoKempner, M., Anderson, D. N., Stewart, F. G., and Perry, J.: Improving ionospheric maps using theoretically derived values of *fo*F2, Radio Sci., 18, 95–107, 1983.

Rush, C. M., PoKempner, M., Anderson, D. N., Perry, J., Stewart, F. G., and Reasoner, R.: Maps of *fo*F2 derived from observations and theoretical data, Radio Sci., 19, 1083–1097. 1984.

Schirliess, I. and Fejer, B. G.: Radar and satellite global equatorial F region vertical drift model, J. Geophys. Res., 104A, 6829–6842, 1999.

Su, Y. Z., Oyama, K.-I., Bailey, G. J., Fukao, S., Takahashi, T., and Oya, H.: Longitudinal variations of the topside ionosphere at low latitudes: Satellite measurements and mathematical modeling, J. Geophys. Res., 101A, 17 191–17 205, 1996.

Thomas, L.: The F2-region equatorial anomaly during solstice periods at sunspot maximum, J. Atmos. Terr. Phys., 30, 1631–1640, 1968.

Walker, G. O.: Longitudinal structure of the F-region equatorial anomaly – a review, J. Atmos. Terr. Phys., 43, 763–774, 1981.